Decay of a single photon in a cavity with atomic mirrors

Chaofan Zhou,[1] Zeyang Liao,[2] and M. Suhail Zubairy[1]
[1]*Institute for Quantum Science and Engineering (IQSE) and Department of Physics and Astronomy, Texas A&M University, College Station, Texas 77843-4242, USA*
[2]*School of Physics, Sun Yat-sen University, Guangzhou 510275, People's Republic of China*

(Received 10 September 2021; accepted 22 February 2022; published 3 March 2022)

We study the decay of a single-photon pulse inside a cavity consisting of two atomic mirrors coupled to a one-dimensional waveguide. The finesse of the cavity can be increased with proper choice of coupling strength, cavity length, spontaneous decay rate, and separation between atoms. The loss rate of a single-photon pulse inside the cavity can be decreased with narrower spectrum width and smaller detuning between the photon pulse and the atomic resonance. The decay of a single-photon pulse in the atomic cavity can be significantly slowed down with proper parameters and the increase of the number of atoms within the atomic mirrors.

DOI: 10.1103/PhysRevA.105.033705

I. INTRODUCTION

Photons are ideal carriers of quantum information. The transfer and storage of photons have important applications in quantum information and quantum computation [1–4]. Many-body physics of photons and atoms has attracted a lot of attention since the Dicke super-radiance [5–9]. Due to the enhancement of the atom-photon interaction by the Purcell effect [2] and because the interaction between the emitters mediated by the waveguide is long range [10], waveguide QED plays an important role in manipulating photons in many-body systems [11–13]. Many systems have been proved to be very good one-dimensional waveguides, such as optical nanofibers [14] and photonic crystal with line defects [15].

The propagation of photons in a one-dimensional waveguide coupled to emitters has been extensively studied [13,16–18]. The stationary solution of the photon transport in the waveguide-QED system was first studied by Shen and Fan [19,20] and then a number of different methods to calculate the scattering properties of this system were proposed such as Lippmann-Schwinger scattering theory [21,22], input-output theory [23,24], and diagrammatic approach [25,26]. Similar approaches were developed to solve the transport of a single photon scattered by multiple two-level atoms [27–29]. Considering systems containing photon pulses with finite bandwidth, a time-dependent theory was brought up to solve the dynamics of the single emitter and the evolution of a single-photon pulse [30]. Then the time-dependent solutions of the transportation of single-photon [31–34] and multiphoton pulses [35,36] scattered by an atomic chain were derived. Due to the coherent interference between the incident field and the field reemitted by the emitter, a photon with frequency near resonant to the emitter transition frequency can be reflected with very high probability. It has been experimentally demonstrated that the extinction of a single-photon pulse with finite bandwidth by a single emitter can approach 100% [37,38]. Two atom arrays coupled to a one-dimensional (1D) waveguide can then become a good cavity [39–41] and a single-photon frequency comb can be generated by this kind of atomic cavity [42]. The microscale Fabry-Perot interferometer with high spectral resolution and tunable transmission frequency may also be realized in this system via chiral waveguide-emitter coupling [43].

Since the atom cavity can find important applications in the integrable quantum photonic chip, in this paper, we focus on studying the decay of a single photon inside the cavity with atomic mirrors coupled to a one-dimensional waveguide. We numerically study the results of cavities consisting of atomic mirrors with different numbers of atoms. We illustrate how the finesse of the cavity and the loss rate of the photon are affected by various parameters, including coupling strength, cavity length, spontaneous decay rate, separation between atoms, spectrum width, and smaller detuning between the photon pulse and the atomic resonance. The results here can be useful for realizing waveguide-based quantum devices.

This paper is organized as follows. In Sec. II, we derive the decay of a single-photon pulse in a cavity with two n-atom mirrors coupled to a one-dimensional waveguide. In Secs. III and IV, we numerically study the decay of a single-photon pulse in a cavity with single-atom mirrors and two-atom mirrors, respectively. The effects of the parameters on the cavity finesse and photon loss rate are discussed. In Sec. V, we study the decay of a single-photon pulse in a cavity with multiple-atom mirrors. The effects of the separation between atoms are analyzed.

II. MODEL AND THEORY

We model our system as a cavity with two atomic mirrors consisting of two-level atoms which are coupled to a one-dimensional waveguide. The atom-field system is described by the Hamiltonian in the rotating wave approximation

[33,44],

$$H = \frac{\hbar}{2}\left(\omega_a - i\frac{\gamma}{2}\right)\sum_{j=1}^{N}\sigma_j^z + \hbar\sum_k \omega_k a_k^\dagger a_k + \hbar\sum_{j=1}^{N}\sum_k \left(g_k^j e^{ikr_j}\sigma_j^+ a_k + \text{H.c.}\right), \quad (1)$$

where σ_j^+ and σ_j^- represent the raising and lowering operators of the jth emitter located at r_j. Also, $\sigma_j^z = [\sigma_j^+, \sigma_j^-]$; γ is the spontaneous decay rate of emitters to the nonguided modes, a_k and $a_k^\dagger$ are the annihilation and creation operators, and g_k^j is the coupling strength between the guided mode and the jth emitter. The jth atom is located at the position r_j. In order to apply the linearized dispersion relation, we assume that the atomic transition frequency ω_a is far away from the cutoff frequency of the waveguide and the photonic spectrum is narrow. Thus, $\delta\omega_k = \omega_k - \omega_a = (|k| - k_a)v_g$, where the v_g is the group velocity of the photon pulse [45].

For the single-photon situation, the atom-field quantum state is $|\Psi(t)\rangle = \sum_{j=1}^{N}\alpha_j(t)e^{-i\omega_a t}|e_j, 0\rangle + \sum_k \beta_k(t)e^{-i\omega_k t}|g, 1_k\rangle$, where $\alpha_j(t)$ is the excitation probability of the jth emitter and $\beta_k(t)$ is the photon spectrum. By tracing out the field parts of the Hamiltonian in Eq. (1), the excitation probability of the jth emitter is given by [42]

$$\alpha_j(t) = \frac{v_g}{2\pi}\int_{-\infty}^{\infty}\sum_{l=1}^{N}[M(\delta k)]_{jl}^{-1}A_l(\delta k)e^{-i\delta k v_g t}d\delta k,$$

with

$$M(\delta k) = \frac{\Gamma}{2}\begin{bmatrix} 1 & e^{ikr_{12}} & \cdots & e^{ikr_{1N}} \\ e^{ikr_{21}} & 1 & \cdots & e^{ikr_{2N}} \\ \vdots & \vdots & \ddots & \vdots \\ e^{ikr_{N1}} & e^{ikr_{N2}} & \cdots & 1 \end{bmatrix} + \left(\frac{\gamma}{2} - i\delta k v_g\right)I_N,$$

$$A_j(\delta k) = \alpha_j(0) - i\sqrt{\frac{\Gamma L}{2v_g}}\beta_0(\delta k)e^{ikr_j}, \quad (2)$$

where $r_{ij} = |r_i - r_j|$ is the distance between the ith and the jth emitter, I_N is an N-dimensional identity matrix, $\Gamma = 2L|g_{k_a}|^2/v_g$ is the coupling strength between the atom and the guided photon with L being the quantization length of the guided modes, and $\alpha_j(0)$ and $\beta_0(\delta k)$ are the initial conditions of the jth emitter and the photon spectrum, respectively. The photon spectra of the left and the right propagating modes are [42]

$$\beta_{\delta k}^L(t) = -i\sqrt{\frac{\Gamma v_g}{2L}}\sum_{j=1}^{N}e^{i(k_a+\delta k)r_j}\int_0^t \alpha_j(t')e^{i\delta k v_g t'}dt', \quad (3)$$

$$\beta_{\delta k}^R(t) = \beta_k(0) - i\sqrt{\frac{\Gamma v_g}{2L}}\sum_{j=1}^{N}e^{-i(k_a+\delta k)r_j}\int_0^t \alpha_j(t')e^{i\delta k v_g t'}dt', \quad (4)$$

where $\delta k = |k| - k_a$ with $k < 0$ ($k > 0$) in left (right) propagating modes. By applying Fourier transform on Eqs. (3) and (4), the spatial distributions of the left and the right propagating photon can be derived as shown in the Appendix:

$$\beta_x^L(t) = \frac{1}{\sqrt{2\pi}}e^{-ik_a x}\int_{-\infty}^{\infty}\beta_{\delta k}^L(t)e^{-i\delta k(x+v_g t)}d\delta k = -i\sqrt{\frac{\Gamma\pi}{Lv_g}}e^{-ik_a x}\sum_{j=1}^{N}e^{ik_a r_j}\alpha_j\left(t + \frac{x - r_j}{v_g}\right)\Theta(r_j - x), \quad (5)$$

$$\beta_x^R(t) = \frac{1}{\sqrt{2\pi}}e^{ik_a x}\int_{-\infty}^{\infty}\beta_{\delta k}^R(t)e^{i\delta k(x-v_g t)}d\delta k = (8\pi)^{\frac{1}{4}}\sqrt{\frac{\Delta}{2L}}e^{ik_a x}\exp\left[-\frac{\Delta^2}{4}\left(-v_g t + x - i\frac{2\Delta_d}{\Delta^2}\right)^2\right] - i\sqrt{2\pi}\sqrt{\frac{\Gamma}{2Lv_g}}e^{ik_a x}\sum_{j=1}^{N}e^{-ik_a r_j}\alpha_j\left(t + \frac{r_j - x}{v_g}\right) \times \Theta(x - r_j), \quad (6)$$

where the $\Theta(x)$ is the Heaviside function with $\Theta(x) = 1$ for $x \geqslant 0$ and $\Theta(x) = 0$ for $x < 0$.

It follows from Eqs. (2)–(6) that the probability amplitude inside of the cavity $P(t)$ is given by

$$P(t) = \sum_j |\alpha_j(t)|^2 + \frac{L}{2\pi}\int_{r_l}^{r_r}\left[\left|\beta_x^L(t)\right|^2 + \left|\beta_x^R(t)\right|^2\right]dx, \quad (7)$$

where $r_l(r_r)$ represents the position of the left (right) boundary of the cavity. The first part is the remaining probability amplitude stored in the excited states of the emitters. The second part is the photon propagating inside the cavity, including the left and the right propagating parts. Clearly, the expression of probability amplitude is too complex to analyze. In order to study the effects of parameters on the decay, we make an approximation that the decay of the photon can be treated as a series of separate individual interactions between the photon pulse and each mirror, which has been well studied [33]. The effective reflectivity of the mirrors is denoted as $R_{\delta k}$. Therefore, after N reflection, the probability amplitude that the photon is still inside the cavity is proportional to $R_{\delta k}^N$. In this case, the remaining probability amplitude inside the cavity can be expressed as

$$P(t) = \int_{-\infty}^{\infty}d\delta k|\beta_{\delta k}(0)|^2 R_{\delta k}^{N(t)}, \quad (8)$$

where $N(t)$ means the Nth interaction at time t. Here, $\beta_{\delta k}(0)$ is the initial shape of the photon pulse. With the help of Eq. (8), the effect of various parameters on the cavity decay can be discussed in the following sections.

The single photon is assumed to be initially trapped inside the cavity. It can be achieved by applying an external field on the side of arrays where the photon is coming from. As long as the frequency of the photon is largely detuned from the transition frequency of the atoms, the photon can propagate through the atoms without being scattered. Then it is trapped by turning off the external field before reaching the other mirror.

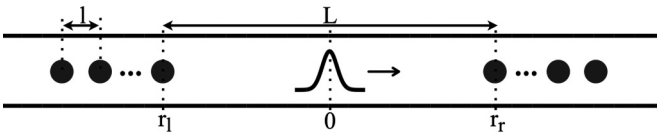

FIG. 1. Atomic cavity with two n-atom mirrors. The photon pulse is initially incident inside the cavity and propagates towards the right as shown. The distance between mirror atoms is l. The distance between two mirrors is L. The emitters are initially in ground states in all the cases.

We study the decay of the single photon inside the cavity with atomic mirrors consisting of one atom, two atoms, and multiple atoms.

III. CAVITY WITH SINGLE-ATOM MIRRORS

In this section, we consider a cavity with two mirrors consisting of one atom each, as shown in Fig. 1. A single-photon pulse is initially incident inside the cavity and propagating towards the right. Thus the photon interacts with the right emitter first. Emitters are initially in ground states, i.e., $\alpha_1(0) = \alpha_2(0) = 0$. Here we take the incident photon pulse as a Gaussian with spectral width Δ, i.e.,

$$\beta_0(\delta k) = \frac{(8\pi)^{1/4}}{\sqrt{\Delta L}} \exp\left[-(\delta k - \Delta_d)^2/\Delta^2\right], \tag{9}$$

where Δ_d is the detuning between the central frequency of the single-photon pulse and the resonance of the emitters. The initial central position of the emitter is r_0. According to Eq. (2), the matrix $M(\delta k)$ and the excitation probabilities of the two mirror atoms are given by

$$M(\delta k) = \frac{\Gamma}{2}\begin{bmatrix} 1 & e^{ikL} \\ e^{ikL} & 1 \end{bmatrix} + \left(\frac{\gamma}{2} - i\delta k v_g\right) I_N, \tag{10}$$

$$\alpha_1(t) = -i\frac{(8\pi)^{\frac{1}{4}}}{\sqrt{2\eta\pi}\,\Delta}\int_{-\infty}^{\infty} d\delta k \frac{-e^{ikL}}{\left(1+\frac{\gamma}{\Gamma}-2i\frac{\delta k v_g}{\Gamma}\right)^2 - e^{2ikL}} \times \exp\left(-\frac{(\delta k-\Delta_d)^2}{\Delta^2} + ikr_2 - i\delta k r_0 - i\delta k v_g t\right), \tag{11}$$

$$\alpha_2(t) = -i\frac{(8\pi)^{\frac{1}{4}}}{\sqrt{2\eta\pi}\,\Delta}\int_{-\infty}^{\infty} d(\delta k) \frac{1+\frac{\gamma}{\Gamma}-2i\frac{\delta k v_g}{\Gamma}}{\left(1+\frac{\gamma}{\Gamma}-2i\frac{\delta k v_g}{\Gamma}\right)^2 - e^{2ikL}} \times \exp\left(-\frac{(\delta k-\Delta_d)^2}{\Delta^2} + ikr_2 - i\delta k r_0 - i\delta k v_g t\right). \tag{12}$$

Since we have $\alpha_j(t) \leqslant 0$ when $t < 0$, the amplitude $\alpha_j(t \pm \frac{x-r_j}{v_g})$ in the spatial distribution of the left (right) propagating part is nonzero when $v_g t \pm (x - r_j) \geqslant 0$. Here, the $+$ and $-$ are for the left and the right propagating parts, respectively. Here we only consider the remaining probability amplitude inside the cavity. Thus, on substituting Eqs. (11) and (12) into Eqs. (5) and (6), the left and right propagating photon pulse shapes within the cavity are

$$\beta_x^L(t) = -i\sqrt{\frac{\Gamma\pi}{Lv_g}} e^{-ik_a x + ik_a r_2}\alpha_2\left(t + \frac{x-r_2}{v_g}\right), \tag{13}$$

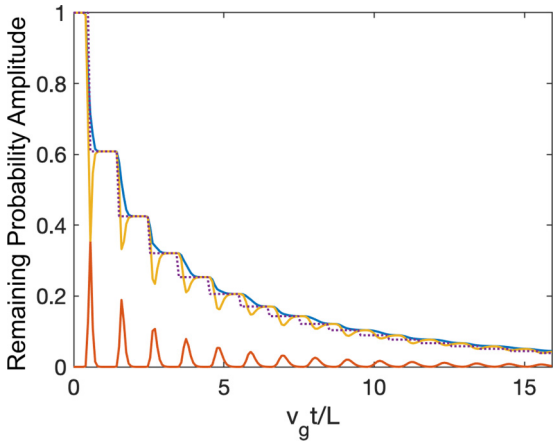

FIG. 2. Decay of a single-photon pulse in the atomic cavity with single-atom mirrors. The remaining probability amplitude is shown inside the cavity (blue, top line), including the propagating part (yellow, middle line) and the part stored in the excited states of the emitters (red, bottom line). The remaining probability amplitude given by the approximation is also shown (dashed line) which separates the process into individual interactions. The cavity length $L = 40\lambda$, where λ represents the wavelength corresponding to the atomic transition frequency ω_a. The Gaussian photon pulse width $\Delta = 0.1k_a$ with no detuning. The spontaneous decay rate to the nonguided modes $\gamma = 0.05\Gamma$.

$$\beta_x^R(t) = (8\pi)^{\frac{1}{4}}\sqrt{\frac{\Delta}{2L}} e^{ik_a x} \exp\left[-\left(-\Delta v_g t + \Delta x - i\frac{2\delta_{af}}{\Delta}\right)^2 \Big/ 4\right] - i\sqrt{\frac{\Gamma\pi}{Lv_g}} e^{ik_a x - ik_a r_1}\alpha_1\left(t + \frac{r_1 - x}{v_g}\right). \tag{14}$$

On substituting $\beta_x^L(t)$ and $\beta_x^R(t)$ from Eqs. (13) and (14) into the definition in Eq. (7), the decay of the single photon can be obtained. The result, when $L = 40\lambda$, $\gamma = 0.05\Gamma$, $\Delta = 0.1k_a$, and $\Delta_d = 0$, is shown in Fig. 2. Here the red solid line is the photon stored in the excited states of all emitters, the yellow solid line is the total propagating photon including both directions, and the blue solid line is the total remaining probability amplitude inside the cavity given by Eq. (7). According to the approximation described in the previous section, the decay can be simplified into a series of individual interactions between the photon pulse and each mirror, which consists of one emitter in this case. The reflectivity due to the interaction between the single atom and single photon is given by $R_{\delta k} = \Gamma^2/[(\Gamma+\gamma)^2 + 4\delta k^2 v_g^2]$ [33].

The remaining probability amplitude with certain wave vector inside the cavity can be written in the form of $R_{\delta k}^{N(t)}$. The propagating time of the photon between the two mirrors is L/v_g. Since we assume the photon is incident in the middle of the cavity, the time-dependent form of $N(t)$ can be written as $[\frac{v_g t}{L} + \frac{1}{2}]$, where $[x]$ is the floor function, i.e., the greatest integer function. As shown in Fig. 2, the purple dashed line is the total remaining probability amplitude inside the cavity given by the approximation described by Eq. (8), i.e.,

$$P(t) = \int_{-\infty}^{\infty} d(\delta k)|\beta_{\delta k}(0)|^2 R^{[\frac{v_g t}{L}+\frac{1}{2}]}. \tag{15}$$

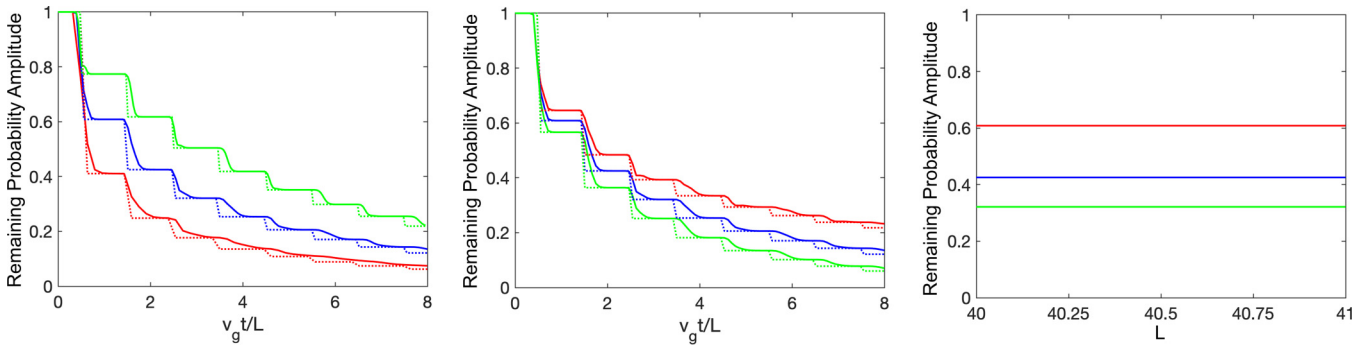

FIG. 3. The effects of the cavity properties on the decay of a single photon in the atomic cavity with single-atom mirrors. Solid lines are the remaining probability amplitude derived from the definition in Eq. (7), while dotted lines are the results of the approximation in Eq. (8). The Gaussian photon pulse with spectrum width $\Delta = 0.1k_a$ and detuning $\Delta_d = 0$ is shown. (a) Comparison of different coupling strengths, $\Gamma = 0.5\Delta v_g, \Delta v_g, 2\Delta v_g$ [red (bottom line), blue (middle line), and green (top line), respectively]. Cavity length $L = 40\lambda$, spontaneous decay rate $\gamma = 0.05\Delta v_g$. (b) Comparison of different spontaneous decay rates, $\gamma = 0.01\Gamma, 0.05\Gamma, 0.1\Gamma$ [red (top line), blue (middle line), and green (bottom line), respectively]. $L = 40\lambda$, $\Gamma = \Delta v_g$. (c) Comparison of different cavity lengths after the first, second, and third interactions [red (top line), blue (middle line), and green (bottom line), respectively]. $\Gamma = \Delta v_g$, $\gamma = 0.05\Gamma$.

Even though the approximation cannot give the exact amount of remaining probability amplitude in arbitrary time, it fits well when the mirror atoms are in the ground states.

The decay rate of the photon inside the cavity is determined by the intrinsic properties of the cavity, including the cavity length L, the coupling strength Γ, and the spontaneous decay rate γ of mirror atoms. In Fig. 3(a), we present the effect of coupling strength Γ of the mirror atoms. The red, blue, and green solid lines represent the results for $\Gamma = 0.5\Delta v_g$, Δv_g, and $2\Delta v_g$, respectively. According to the reflectivity $\Gamma^2/[(\Gamma+\gamma)^2 + 4\delta k^2 v_g^2]$, higher Γ can provide higher reflectivity. Specifically when $\delta k = 0$, the reflectivity for the resonant mode reaches the maximum. Two mirrors with higher reflectivity can form a cavity with higher finesse. In Fig. 3(b), a comparison of the decay of the photon in cavities with different spontaneous decay rates is presented. The red, blue, and green solid lines represent the results of $\gamma = 0.01\Gamma, 0.05\Gamma$, and 0.1Γ, respectively. Higher γ means faster decay due to the spontaneous emission into nonguided modes when the mirror atoms are in the excited states. Nonguided photons are not considered here. Thus the higher spontaneous decay rate causes lower cavity finesse. In certain waveguides, Γ can be much greater than the spontaneous emission rate. For example, in a photonic crystal waveguide, 99% of the collection efficiency of a photon into the waveguide was achieved, which indicates that the Γ is 99 times the γ [38]. Next we consider the effect of the cavity length. It is obvious that larger cavity length can lower the photon loss rate by lowering the frequency of interactions between the photon pulse and the atomic mirrors. So we choose $v_g t/L$ as the timescale to rule out the effect of the magnitude of the cavity length. In Fig. 3(c), the red, blue, and green solid lines represent the probability amplitude after the first, second, and third interactions, respectively, with cavity length L ranging from 40λ to 41λ. The remaining probability amplitude is not influenced in the timescale $v_g t/L$, i.e., the photon lost in each interaction is independent of the length of the cavity.

Since we consider the incident photon with Gaussian shape, the decay rate of the photon inside the cavity is also determined by the parameters of the photon pulse, including the spectral width Δ and the detuning Δ_d. As shown in Fig. 4(a), we compare the decay of the photon with different spectral width Δ. The red, blue, and green solid lines represent the results of $\Delta = 0.05k_a, 0.1k_a$, and $0.2k_a$. In Fig. 4(b), we show the effect of detuning Δ_d. The red, blue, and green solid lines represent the results of $\Delta_d = 0, 0.5\Delta$, and 1Δ, respectively. The reflectivity $\Gamma^2/[(\Gamma+\gamma)^2 + 4\delta k^2 v_g^2]$ indicates that modes with smaller δk can lead to larger reflectivity. Higher Δ means that the spectral distribution is more dispersed around $\delta k = 0$. Larger Δ_d shifts the center further away from $\delta k = 0$. Both cases cause lower reflectivity of the mirror and lower cavity finesse.

IV. CAVITY WITH TWO-ATOM MIRRORS

In this section, we consider the decay of a single-photon pulse in a cavity which consists of two two-atom mirrors. Within the mirror, the distance between atoms is l. The separation between mirrors is L. All four emitters are initially in ground states, i.e., $\alpha_j(0) = 0$. The photon pulse is initially incident in the middle of the cavity. It propagates towards the right as shown.

According to Eq. (2), the matrix $M(\delta k)$ and the amplitude $\alpha_j(t)$ are given by

$$M(\delta k) = \frac{\Gamma}{2}\begin{bmatrix} 1 & e^{ikl} & e^{ik(l+L)} & e^{ik(2l+L)} \\ e^{ikl} & 1 & e^{ikL} & e^{ik(l+L)} \\ e^{ik(l+L)} & e^{ikL} & 1 & e^{ikl} \\ e^{ik(2l+L)} & e^{ik(l+L)} & e^{ikl} & 1 \end{bmatrix} + \left(\frac{\gamma}{2} - i\delta k v_g\right) I_N, \tag{16}$$

$$\alpha_j(t) = \frac{v_g}{2\pi}\int_{-\infty}^{\infty} \sum_{k=3,4} [M(\delta k)]^{-1}_{jl} b_l(\delta k) e^{-i\delta k v_g t} d\delta k. \tag{17}$$

The photon pulse shape can be calculated by substituting $\alpha_j(t)$ into Eqs. (5) and (6). Then the probability amplitude

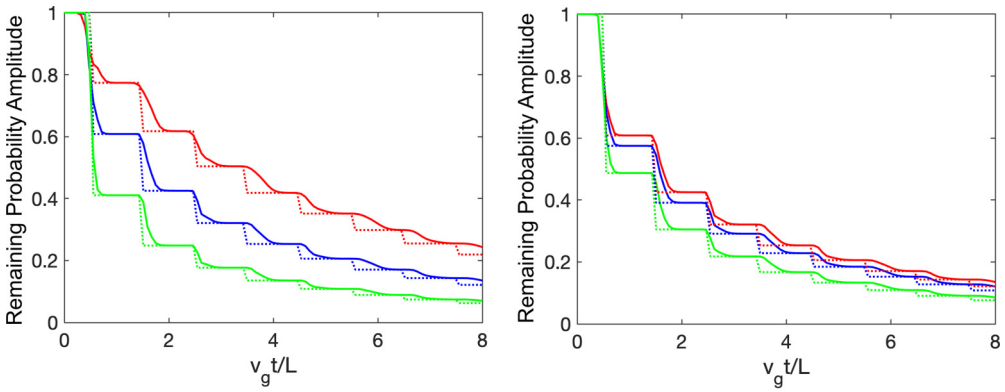

FIG. 4. The effects of the photon pulse properties on the decay of a single photon in the atomic cavity with single-atom mirrors. Solid lines are the remaining probability amplitude derived from the definition in Eq. (7), while dotted lines are the results of the approximation in Eq. (8). The cavity with $L = 40\lambda$, $\Gamma = \Delta v_g$, $\gamma = 0.05\Gamma$. (a) Comparison of different Gaussian pulse spectra with $\Delta = 0.05k_a, 0.1k_a, 0.2k_a$ [red (top line), blue (middle line), and green (bottom line), respectively]. Detuning $\Delta_d = 0$. (b) Comparison of different detunings, $\Delta_d = 0, 0.5\Delta, 1\Delta$ [red (top line), blue (middle line), and green (bottom line), respectively]. $\Delta = 0.1k_a$

inside the cavity is obtained by the definition in Eq. (7). The result when $l = 1\lambda$, $L = 40\lambda$, $\Gamma = \Delta v_g$, $\gamma = 0.05\Gamma$, $\Delta = 0.1k_a$, and $\Delta_d = 0$ is shown in Fig. 5. Here the red solid line is the probability amplitude stored in the excited states of all emitters, the yellow solid line is the total propagating photon amplitude including both directions, and the blue solid line is the remaining photon pulse inside the cavity given by Eq. (7). The reflectivity of the interaction between a two-atom mirror and the single photon is known as [42]

$$R = \left| \frac{\eta_\Gamma (1 + e^{2ika})(1 - i\eta_{\delta k}) - 2\eta_\Gamma^2 e^{2ika}}{(1 - i\eta_{\delta k})^2 - \eta_\Gamma^2 e^{2ika}} \right|^2, \tag{18}$$

where $\eta_\Gamma = \frac{\Gamma}{\Gamma+\gamma}$, $\eta_{\delta k} = \frac{2\delta k v_g}{\Gamma+\gamma}$. Again, as shown in Fig. 5, the approximation fits well with the results when emitters are in the ground states.

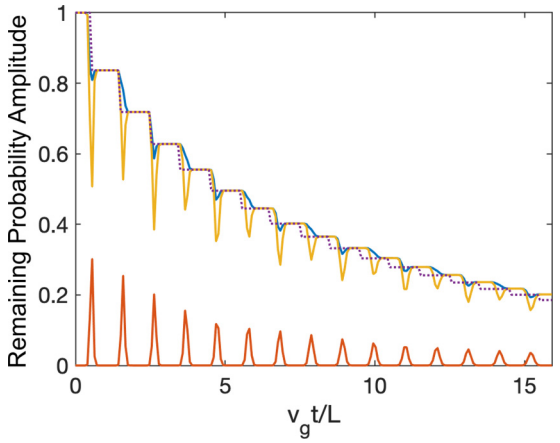

FIG. 5. Decay of a single-photon pulse in the atomic cavity with two-atom mirrors. The total remaining probability amplitude inside the cavity is also shown. The red line (bottom) represents the excitation probability of the emitters. The yellow line (middle) is the propagating photon amount. The blue line (top) is the remaining probability amplitude inside the cavity, including the propagating part and the part stored in the excited states of the mirror atoms. The purple dashed line is the remaining probability amplitude given by the approximation which separates the process into individual interactions between the photon pulse single atom. The cavity length $L = 40\lambda$. The Gaussian photon pulse width $\Delta = 0.1k_a$ with no detuning. The spontaneous decay rate to the nonguided modes $\gamma = 0.1\Gamma$.

The parameters of the cavity have similar effects as discussed in the previous section. In Figs. 6(a) and 6(b), it is shown that higher coupling strength Γ and lower spontaneous decay rate γ help decrease the cavity loss rate. The dashed lines are the result of a cavity with single-atom mirrors with the same cavity properties, except for the separation l within the mirrors. It shows that a cavity with two-atom mirrors has better finesse. By ruling out the influence of the magnitude of the cavity length, the loss of the photon in interactions with the mirrors is not affected in timescale $v_g t/L$, as shown in Fig. 6(c). However, the separation between atoms l can change the cavity finesse. The remaining probability amplitude, as a function of l, is shown in Fig. 6(d), where the maximal finesse can be found when $l = \lambda/2, \lambda$. The parameters of the Gaussian photon pulse have similar effects in the two-atom mirror case as well. As shown in Figs. 6(e) and 6(f), smaller spectrum width Δ and detuning Δ_d lead to a lower photon loss rate since the reflectivity increases in both ways.

In Figs. 6(a)–6(f), the dashed lines represent the results of a cavity with single-atom mirrors with the same parameters, including cavity length, coupling strength, and spontaneous decay rate. A cavity with two-atom mirrors lowers the photon loss rate and extends the time of the single-photon pulse being stored in the cavity.

V. CAVITY WITH *N*-ATOM MIRRORS

The decay of a single photon in a cavity with N-atom mirrors can be obtained by Eq. (7) as shown in previous sections. Generally speaking, mirrors with more atoms can

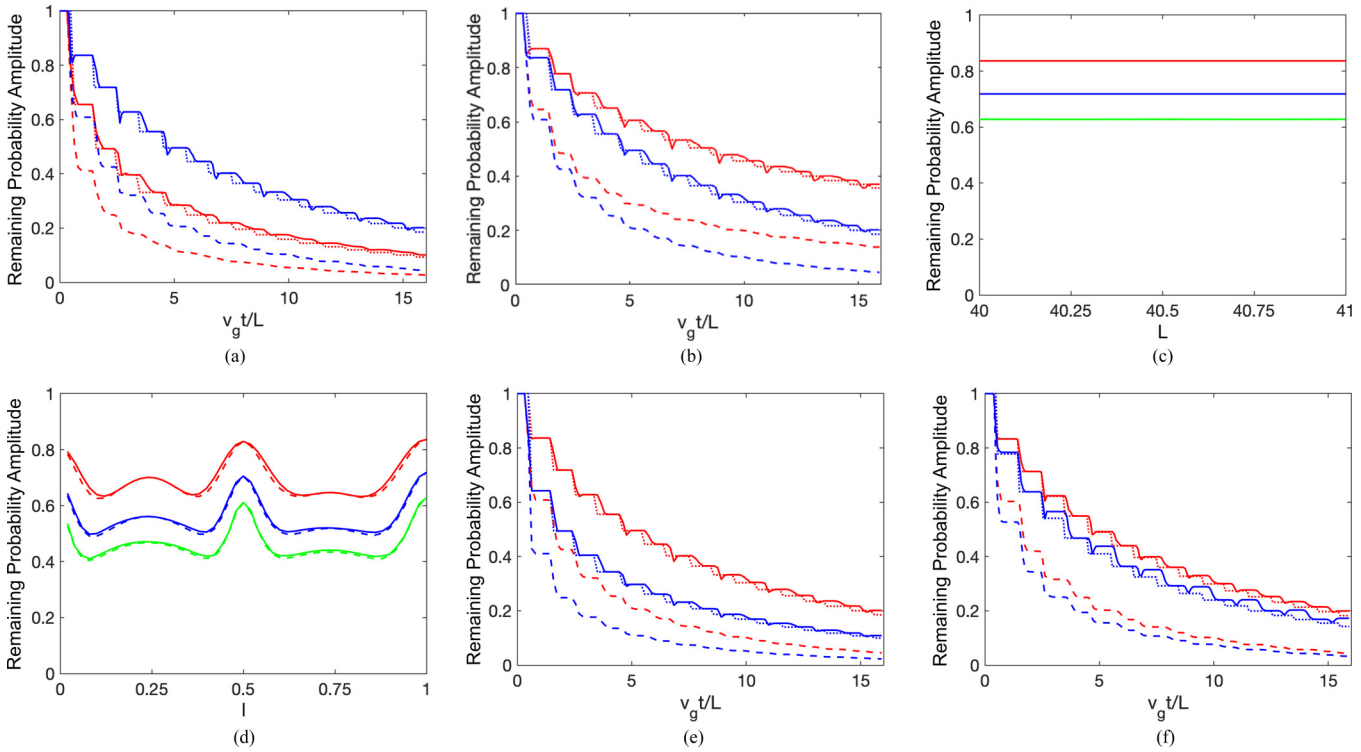

FIG. 6. (a)–(d) The effects of the cavity properties on the decay of a single photon in the atomic cavity with two-atom mirrors. Solid lines are the probability amplitude derived from the definition in Eq. (7), while dotted lines are the results of the approximation in Eq. (8). Dashed lines are the results of a cavity with single-atom mirrors. The Gaussian photon pulse with spectrum width $\Delta = 0.1k_a$ and detuning $\Delta_d = 0$. (a) Comparison of different coupling strengths, $\Gamma = 0.5\Delta v_g$, Δv_g [red (bottom line) and blue (top line), respectively]. The cavity length $L = 40\lambda$, separation $l = \lambda$, and spontaneous decay rate $\gamma = 0.05\Delta v_g$. (b) Comparison of different spontaneous decay rates, $\gamma = 0.01\Gamma$, 0.05Γ [red (top line) and blue (bottom line), respectively]. $L = 40\lambda$, $l = \lambda$, $\Gamma = \Delta v_g$. (c) Comparison of different cavity lengths after the first, second, and third interactions [red (top line), blue (middle line), and green (bottom line), respectively]. $l = \lambda$, $\Gamma = \Delta v_g$, $\gamma = 0.05\Gamma$. (d) Comparison of different separations within mirrors after the first, second, and third interactions [red (top line), blue (middle line), and green (bottom line), respectively]. $L = 40\lambda$, $\Gamma = \Delta v_g$, $\gamma = 0.05\Gamma$. (e),(f) The effects of the photon pulse properties on the decay of a single photon in the atomic cavity with single-atom mirrors. Solid lines are the probability amplitudes derived from the definition in Eq. (7), while dotted lines are the results of the approximation in Eq. (8). Dashed lines are the results of a cavity with single-atom mirrors. The cavity with $L = 40\lambda$, $l = \lambda$, $\Gamma = \Delta v_g$, $\gamma = 0.05\Gamma$. (e) Comparison of different Gaussian pulse spectra with $\Delta = 0.1k_a$, $0.2k_a$ [red (top line) and blue (bottom line), respectively]. Detuning $\Delta_d = 0$. (f) Comparison of different detunings, $\Delta_d = 0.1\Delta$, 0.5Δ [red (top line) and blue (bottom line), respectively]. $\Delta = 0.1k_a$.

provide higher reflectivity, which leads to a smaller photon loss rate.

As shown in Figs. 7(a)–7(c), separation $l = \lambda/2$ (black line) provides better reflectivity than $l = \lambda/4$ (red line) and $\lambda/8$ (blue line) in all the cases with multiple-atom mirrors, which accords with the results from Fig. 6(d). In Fig. 7(d), we illustrate the effects of atomic separation on the reflectivity. The mirrors with on-resonance atomic separations, i.e., $l = n\lambda/2$, provide wider photonic band gaps and higher reflectivity, which guarantees better finesse. Considering nonidentical

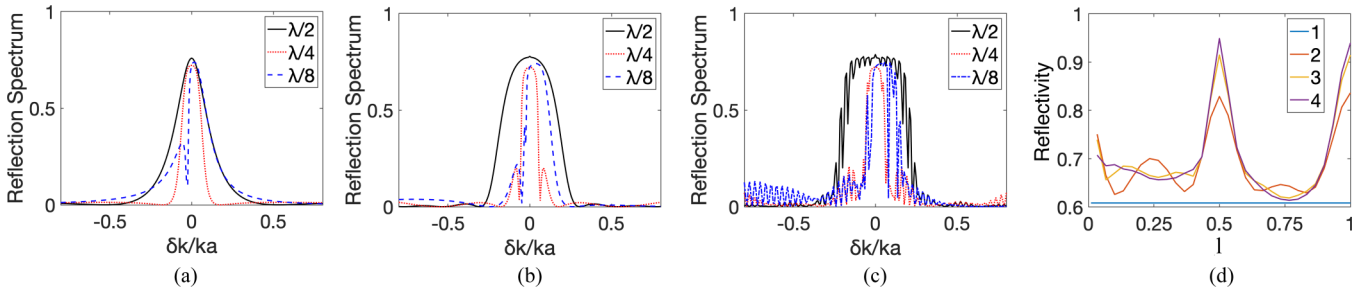

FIG. 7. The reflection spectrum of a (a) two-, (b) three-, and (c) four-atom mirror with separation $l = \lambda/2$ (black solid line), $\lambda/4$ (red dotted line), and $\lambda/8$ (blue dashed line). (d) The reflectivity varies with different separations l within atomic mirrors consisting of one (blue line), two (red line), three (yellow line), and four (purple line) atoms.

emitters, it has been demonstrated that the randomness of parameters affects the reflection spectrum, for example, the atomic transition frequency variation [34]. It shows that if the energy differences of the emitters are large, far-off-resonant atoms can be treated as absent. Less atoms will lead to a higher decay rate. If the energy differences of the emitters are relatively small and nonzero, a very narrow transmission window appears around the resonance frequency, which is called dipole-dipole-induced electromagnetic transparency (DIET). The transmission window also gives a higher decay rate of photons with some narrow frequency bands.

With proper choices of atomic separation, the reflection spectrum would be broadened due to the collective interaction effects. Higher reflectivity can be achieved considering the same photon pulse, even with other different shapes, e.g., the Lorentzian shape. In the above discussions, the atom chain is assumed to be uniform. Although the spatial disorder and inhomogeneity of the atomic parameters can affect the reflectivity of the photon pulse, the overall qualitative results are similar to the case we discussed above.

VI. SUMMARY

In summary, we study the decay of a single-photon pulse in a cavity consisting of two atomic mirrors, which are coupled to a 1D waveguide. The properties of the cavities, including coupling strength, cavity length, spontaneous decay rate, and separation between atoms, affect the finesse of the cavity. The parameters of the photon pulses, including spectrum width and detuning, affect the loss rate of a single-photon pulse inside the cavity. The results can be applied to help with the storage of a single-photon pulse. With proper choice of parameters, the time of a single-photon pulse being stored in the cavity can be significantly extended. The results found here might help to engineer microscale cavities with high-quality factors which can be used for integrable quantum devices and a high-resolution waveguide-QED-based spectrometer. In addition, a high-finesse cavity can also help to realize a single-atom laser in the waveguide systems.

ACKNOWLEDGMENTS

This research is supported by Project No. NPRP 13S-0205-200258 of the Qatar National Research Fund (QNRF). C.Z. is supported by the HEEP Fellowship. Z.L. is supported by the Natural Science Foundations of Guangdong (Grant No. 2021A1515010039) and the Fundamental Research Funds for the Central Universities, Sun Yat-sen University (Grant No. 2021qntd27).

APPENDIX

Through substituting Eq. (3) into the Fourier transform in Eq. (5),

$$\beta_x^L(t) = \frac{1}{\sqrt{2\pi}} e^{-ik_a x} \int_{-\infty}^{\infty} d\delta k \beta_{\delta k}^L(t) e^{-i\delta k(x+v_g t)} \tag{A1}$$

$$= \frac{1}{\sqrt{2\pi}} e^{-ik_a x} \int_{-\infty}^{\infty} d\delta k \left(-i\sqrt{\frac{\Gamma v_g}{2L}} \right) \sum_{j=1}^{N} e^{i(k_a+\delta k)r_j} \int_0^t dt' \alpha_j(t') e^{i\delta k v_g t'} e^{-i\delta k(x+v_g t)} \tag{A2}$$

$$= -i\frac{1}{\sqrt{2\pi}} \sqrt{\frac{\Gamma v_g}{2L}} e^{-ik_a x} \sum_{j=1}^{N} e^{ik_a r_j} \int_{-\infty}^{\infty} d\delta k \int_0^t dt' e^{i\delta k(r_j + v_g t' - x - v_g t)} \alpha_j(t') \tag{A3}$$

$$= -i\frac{1}{\sqrt{2\pi}} \sqrt{\frac{\Gamma v_g}{2L}} e^{-ik_a x} \sum_{j=1}^{N} e^{ik_a r_j} 2\pi \int_0^t dt' \delta(r_j + v_g t' - x - v_g t) \alpha_j(t') \tag{A4}$$

$$= -i\sqrt{\frac{\Gamma\pi}{L v_g}} e^{-ik_a x} \sum_{j=1}^{N} e^{ik_a r_j} \alpha_j\left(t + \frac{x - r_j}{v_g}\right) \Theta(r_j - x). \tag{A5}$$

Similarly, substituting Eq. (4) into the Fourier transform in Eq. (6),

$$\beta_x^R(t) = \frac{1}{\sqrt{2\pi}} e^{ik_a x} \int_{-\infty}^{\infty} d\delta k \beta_{\delta k}^R(t) e^{i\delta k(x - v_g t)} \tag{A6}$$

$$= \frac{1}{\sqrt{2\pi}} e^{ik_a x} \int_{-\infty}^{\infty} d\delta k \beta_{\delta k}(0) e^{i\delta k(x - v_g t)} + \frac{1}{\sqrt{2\pi}} e^{ik_a x} \int_{-\infty}^{\infty} d\delta k \left(-i\sqrt{\frac{\Gamma v_g}{2L}} \right) \sum_{j=1}^{N} e^{-i(k_a+\delta k)r_j} \int_0^t dt' \alpha_j(t') e^{i\delta k v_g t'} e^{i\delta k(x - v_g t)} \tag{A7}$$

$$= \frac{1}{\sqrt{2\pi}} e^{ik_a x} \int_{-\infty}^{\infty} d\delta k \beta_{\delta k}(0) e^{i\delta k(x - v_g t)} - i\sqrt{\frac{\Gamma\pi}{L v_g}} e^{ik_a x} \sum_{j=1}^{N} e^{-ik_a r_j} \int_{-\infty}^{\infty} d\delta k \int_0^t dt' e^{i\delta k(-r_j + v_g t' + x - v_g t)} \alpha_j(t') \tag{A8}$$

$$= \frac{1}{\sqrt{2\pi}} e^{ik_a x} \int_{-\infty}^{\infty} d\delta k \beta_{\delta k}(0) e^{i\delta k(x - v_g t)} - i\sqrt{\frac{\Gamma\pi}{L v_g}} e^{ik_a x} \sum_{j=1}^{N} e^{-ik_a r_j} 2\pi \int_0^t dt' \delta(-r_j + v_g t' + x - v_g t) \alpha_j(t') \tag{A9}$$

$$= \frac{1}{\sqrt{2\pi}} e^{ik_a x} \int_{-\infty}^{\infty} d\delta k \beta_{\delta k}(0) e^{i\delta k(x - v_g t)} - i\sqrt{\frac{\Gamma\pi}{L v_g}} e^{ik_a x} \sum_{j=1}^{N} e^{-ik_a r_j} \alpha_j \left(t + \frac{r_j - x}{v_g}\right) \Theta(x - r_j) \tag{A10}$$

$$= (8\pi)^{\frac{1}{4}} \sqrt{\frac{\Delta}{2L}} e^{ik_a x} \exp\left[-\left(-\Delta v_g t + \Delta x - i\frac{2\delta_{af}}{\Delta}\right)^2 \Big/ 4\right] - i\sqrt{\frac{\Gamma\pi}{L v_g}} e^{ik_a x} \sum_{j=1}^{N} e^{-ik_a r_j} \alpha_j \left(t + \frac{r_j - x}{v_g}\right) \Theta(x - r_j). \tag{A11}$$

[1] J. M. Raimond, M. Brune, and S. Haroche, Manipulating quantum entanglement with atoms and photons in a cavity, Rev. Mod. Phys. **73**, 565 (2001).

[2] E. M. Purcell, H. C. Torrey, and R. V. Pound, Resonance absorption by nuclear magnetic moments in a solid, Phys. Rev. **69**, 37 (1946).

[3] J. Hwang, M. Pototschnig, R. Lettow, G. Zumofen, A. Renn, S. Götzinger, and V. Sandoghdar, A single-molecule optical transistor, Nature (London) **460**, 76 (2009).

[4] Z. Tian, P. Zhang, and X.-W. Chen, Static Hybrid Quantum Nodes: Toward Perfect State Transfer on a Photonic Chip, Phys. Rev. Appl. **15**, 054043 (2021).

[5] R. H. Dicke, Coherence in spontaneous radiation processes, Phys. Rev. **93**, 99 (1954).

[6] N. Skribanowitz, I. P. Herman, J. C. MacGillivray, and M. S. Feld, Observation of Dicke Superradiance in Optically Pumped hf Gas, Phys. Rev. Lett. **30**, 309 (1973).

[7] M. Gross and S. Haroche, Superradiance: An essay on the theory of collective spontaneous emission, Phys. Rep. **93**, 301 (1982).

[8] M. O. Scully and A. A. Svidzinsky, The super of superradiance, Science **325**, 1510 (2009).

[9] A. A. Svidzinsky, J.-T. Chang, and M. O. Scully, Cooperative spontaneous emission of n atoms: Many-body eigenstates, the effect of virtual Lamb shift processes, and analogy with radiation of n classical oscillators, Phys. Rev. A **81**, 053821 (2010).

[10] Y. Yu, F. Ma, X.-Y. Luo, B. Jing, P.-F. Sun, R.-Z. Fang, C.-W. Yang, H. Liu, M.-Y. Zheng, X.-P. Xie *et al.*, Entanglement of two quantum memories via fibres over dozens of kilometres, Nature (London) **578**, 240 (2020).

[11] D. Roy, C. M. Wilson, and O. Firstenberg, Colloquium: Strongly interacting photons in one-dimensional continuum, Rev. Mod. Phys. **89**, 021001 (2017).

[12] X. Gu, A. F. Kockum, A. Miranowicz, Y.-X. Liu, and F. Nori, Microwave photonics with superconducting quantum circuits, Phys. Rep. **718**, 1 (2017).

[13] M.-T. Cheng, J. Xu, and G. S. Agarwal, Waveguide transport mediated by strong coupling with atoms, Phys. Rev. A **95**, 053807 (2017).

[14] B. Dayan, A. S. Parkins, T. Aoki, E. P. Ostby, K. J. Vahala, and H. J. Kimble, A photon turnstile dynamically regulated by one atom, Science **319**, 1062 (2008).

[15] D. Englund, A. Faraon, B. Zhang, Y. Yamamoto, and J. Vučković, Generation and transfer of single photons on a photonic crystal chip, Opt. Express **15**, 5550 (2007).

[16] Z. Liao, X. Zeng, H. Nha, and M. S. Zubairy, Photon transport in a one-dimensional nanophotonic waveguide QED system, Phys. Scr. **91**, 063004 (2016).

[17] L.-H. Chen, G. Chen, R. Liu, and X.-H. Wang, Dynamically tunable multifunctional QED platform, Sci. China Phys. Mech. Astron. **62**, 1 (2019).

[18] E. Kim, X. Zhang, V. S. Ferreira, J. Banker, J. K. Iverson, A. Sipahigil, M. Bello, A. González-Tudela, M. Mirhosseini, and O. Painter, Quantum Electrodynamics in a Topological Waveguide, Phys. Rev. X **11**, 011015 (2021).

[19] J. T. Shen and S. Fan, Coherent photon transport from spontaneous emission in one-dimensional waveguides, Opt. Lett. **30**, 2001 (2005).

[20] J. T. Shen and S. Fan, Coherent Single Photon Transport in a One-Dimensional Waveguide Coupled with superconducting Quantum Bits, Phys. Rev. Lett. **95**, 213001 (2005).

[21] D. Roy, Correlated few-photon transport in one-dimensional waveguides: Linear and nonlinear dispersions, Phys. Rev. A **83**, 043823 (2011).

[22] J.-F. Huang, T. Shi, C. P. Sun, and F. Nori, Controlling single-photon transport in waveguides with finite cross section, Phys. Rev. A **88**, 013836 (2013).

[23] S. Fan, Ş. E. Kocabaş, and J.-T. Shen, Input-output formalism for few-photon transport in one-dimensional nanophotonic waveguides coupled to a qubit, Phys. Rev. A **82**, 063821 (2010).

[24] A. H. Kiilerich and K. Mølmer, Input-Output Theory with Quantum Pulses, Phys. Rev. Lett. **123**, 123604 (2019).

[25] T. Shi and C. P. Sun, Lehmann-Symanzik-Zimmermann reduction approach to multiphoton scattering in coupled-resonator arrays, Phys. Rev. B **79**, 205111 (2009).

[26] F. Dinc, Diagrammatic approach for analytical non-Markovian time evolution: Fermi's two-atom problem and causality in waveguide quantum electrodynamics, Phys. Rev. A **102**, 013727 (2020).

[27] J.-T. Shen and S. Fan, Strongly Correlated Two-Photon Transport in a One-Dimensional Waveguide Coupled to a Two-Level System, Phys. Rev. Lett. **98**, 153003 (2007).

[28] T. S. Tsoi and C. K. Law, Quantum interference effects of a single photon interacting with an atomic chain inside a one-dimensional waveguide, Phys. Rev. A **78**, 063832 (2008).

[29] D. Roy, Cascaded two-photon nonlinearity in a one-dimensional waveguide with multiple two-level emitters, Sci. Rep. **3**, 2337 (2013).

[30] Y. Chen, M. Wubs, J. Mørk, and A. F. Koenderink, Coherent single-photon absorption by single emitters coupled to one-dimensional nanophotonic waveguides, New J. Phys. **13**, 103010 (2011).

[31] P. Domokos, P. Horak, and H. Ritsch, Quantum description of light-pulse scattering on a single atom in waveguides, Phys. Rev. A **65**, 033832 (2002).

[32] O. O. Chumak and E. V. Stolyarov, Phase-space distribution functions for photon propagation in waveguides coupled to a qubit, Phys. Rev. A **88**, 013855 (2013).

[33] Z. Liao, X. Zeng, S.-Y. Zhu, and M. S. Zubairy, Single-photon transport through an atomic chain coupled to a one-dimensional nanophotonic waveguide, Phys. Rev. A **92**, 023806 (2015).

[34] Z. Liao, H. Nha, and M. S. Zubairy, Dynamical theory of single-photon transport in a one-dimensional waveguide coupled to identical and nonidentical emitters, Phys. Rev. A **94**, 053842 (2016).

[35] Z. Liao, Y. Lu, and M. S. Zubairy, Multiphoton pulses interacting with multiple emitters in a one-dimensional waveguide, Phys. Rev. A **102**, 053702 (2020).

[36] A. Carmele, N. Nemet, V. Canela, and S. Parkins, Pronounced non-Markovian features in multiply excited, multiple emitter waveguide QED: Retardation induced anomalous population trapping, Phys. Rev. Research **2**, 013238 (2020).

[37] I.-C. Hoi, C. M. Wilson, G. Johansson, T. Palomaki, B. Peropadre, and P. Delsing, Demonstration of a Single-Photon Router in the Microwave Regime, Phys. Rev. Lett. **107**, 073601 (2011).

[38] L. Scarpelli, B. Lang, F. Masia, D. M. Beggs, E. A. Muljarov, A. B. Young, R. Oulton, M. Kamp, S. Höfling, C. Schneider *et al.*, 99% beta factor and directional coupling of quantum dots to fast light in photonic crystal waveguides determined by spectral imaging, Phys. Rev. B **100**, 035311 (2019).

[39] L. Zhou, H. Dong, Y.-X. Liu, C. P. Sun, F. Nori *et al.*, Quantum supercavity with atomic mirrors, Phys. Rev. A **78**, 063827 (2008).

[40] D. E. Chang, L. Jiang, A. V. Gorshkov, and H. J. Kimble, Cavity QED with atomic mirrors, New J. Phys. **14**, 063003 (2012).

[41] M. Mirhosseini, E. Kim, X. Zhang, A. Sipahigil, P. B. Dieterle, A. J. Keller, A. Asenjo-Garcia, D. E. Chang, and O. Painter, Cavity quantum electrodynamics with atom-like mirrors, Nature (London) **569**, 692 (2019).

[42] Z. Liao, H. Nha, and M. S. Zubairy, Single-photon frequency-comb generation in a one-dimensional waveguide coupled to two atomic arrays, Phys. Rev. A **93**, 033851 (2016).

[43] Y. Lu, S. Gao, A. Fang, Z. Liao, and F. Li, Micro-scale Fabry-Perot interferometer with high spectral resolution and tunable transmission frequency via chiral waveguide-emitter coupling, Phys. Lett. A **382**, 1823 (2018).

[44] M. O. Scully and M. S. Zubairy, *Quantum Optics* (Cambridge University Press, Cambridge, 2001).

[45] J.-T. Shen and S. Fan, Theory of single-photon transport in a single-mode waveguide. I. Coupling to a cavity containing a two-level atom, Phys. Rev. A **79**, 023837 (2009).